Kinetics of the Reduction of Co(*o*-phen)$_3^{3+}$ by the Metal Carbonyl Anions Re(CO)$_5^-$, Mn(CO)$_4$L$^-$ (L = CO, PEt$_3$, PBu$_3$, PPh$_3$), Co(CO)$_4^-$, CpMo(CO)$_3^-$, and CpFe(CO)$_2^-$ (Cp = η^5-C$_5$H$_5$, *o*-phen = *o*-Phenanthroline). Structural Determinations of [PPN$^+$][Mn(CO)$_5^-$] and [PPN$^+$][Mn(CO)$_4$(PEt$_3$)$^-$]·THF

M. Shauna Corraine, C. K. Lai, Yueqian Zhen, Melvyn Rowen Churchill,* Lisa A. Buttrey, Joseph W. Ziller,† and Jim D. Atwood*

Department of Chemistry, University at Buffalo, State University of New York, Buffalo, New York 14214

Received May 24, 1991

Reaction of metal carbonyl anions, [M$^-$], with M′(*o*-phen)$_3^{3+}$ (M′ = Fe, Co) results in electron transfer giving metal carbonyl dimers and M(*o*-phen)$_3^{2+}$. The rate depends on the concentration of M′(*o*-phen)$_3^{3+}$ and on [M$^-$]. Fe(*o*-phen)$_3^{3+}$ reacts much more rapidly than does Co(*o*-phen)$_3^{3+}$, consistent with expectations for an outer-sphere electron-transfer process. Dependence on the nature of the metal carbonyl anions is also consistent with outer-sphere electron transfer. Reaction of the metal carbonyl anions with 3-acetoxy-*N*-methylpyridinium tetrafluoroborate is also used to show the outer-sphere reactivity of the metal carbonyl anions. Structures of the PPN$^+$ salts of the Mn(CO)$_4$L$^-$ anions (L = CO and PEt$_3$) are reported as a possible means to assess intrinsic barriers. [PPN$^+$][Mn(CO)$_5^-$], space group $P\bar{1}$, a = 11.339 (2) Å, b = 11.579 (2) Å, c = 14.540 (3) Å, α = 77.030 (12)°, β = 77.553 (13)°, γ = 89.530 (13)°, V = 1814.9 (5) Å^3, Z = 2; R_F = 6.2% for all 4374 data and 3.7% for those 3088 data with $|F_o| > 6.0\sigma(|F_o|)$. [PPN$^+$][Mn(CO)$_4$(PEt$_3$)$^-$]·THF, space group $P\bar{1}$, a = 9.216 (2) Å, b = 14.059 (3) Å, c = 18.418 (5) Å, α = 96.875 (19)°, β = 93.274 (18)°, γ = 94.497 (17)°, V = 2356.7 (9) Å^3, Z = 2; R_F = 6.1% for 4790 data with $|F_o| > 3.0\sigma(|F_o|)$ and 5.1% for those 4101 data with $|F_o| > 6.0\sigma(|F_o|)$.

Electron-transfer reactions between coordination complexes have been extensively studied and are reasonably well understood.[1-3] There have been relatively few investigations of electron-transfer reactions between coordination complexes and organometallic complexes other than ferrocene.[4] Oxidations of several metal carbonyl dimers have been reported.[5] The oxidation of Cp$_2$Fe$_2$(CO)$_4$ by Ru(bpy)$_2$Cl$_2^+$ was reported to involve an outer-sphere transfer of an electron from the Fe–Fe bond to the ruthenium atom.[5a]

The reactions of metal carbonyl anions with M(*o*-phen)$_3^{3+}$ occur cleanly, giving the electron-transfer products.

$$2M^- + 2M'(o\text{-phen})_3^{3+} \rightarrow M_2 + 2M'(o\text{-phen})_3^{2+} \quad (1)$$

M = metal carbonyl, M′ = Co, Fe

The tris(*o*-phenanthroline) complexes are known to be electron acceptors through an outer-sphere mechanism. Thus this examination defining the outer-sphere electron-transfer reactivity of metal carbonyl anions would augment the growing number of reactions of metal carbonyl anions that occur by an inner-sphere mechanism initiated by nucleophilic attack.[6]

Experimental Section

Materials. All synthetic procedures were carried out under an inert (N$_2$ or argon) atmosphere with glovebox or Schlenk techniques, unless otherwise noted. Solvents were dried by standard procedures. Elemental analyses were performed by Oneida Research Services Inc., NY. Infrared spectra were recorded on a Beckman 4240 infrared spectrophotometer or on a Mattson Polaris FTIR instrument. All chemicals were used as received. [PPN][Cl] (PPN = bis(triphenylphosphine)iminium) was purchased from Strem Chemical. The following compounds were prepared by literature procedures: [PPN][CpFe(CO)$_2$],[7] [PPN][Re(CO)$_5$],[8] [PPN][Mn(CO)$_5$],[7] [PPN][CpMo(CO)$_3$],[7] [PPN][Mn(CO)$_4$L][7] (L = PEt$_3$, PPh$_3$, PBu$_3$). All IR spectra of these compounds (Table S1, supplementary material) were consistent with those reported, and the purities for the kinetic experiments were confirmed by elemental analysis (Table S2, supplementary material).

Tris(1,10-phenanthroline)cobalt(III) perchlorate, [Co(*o*-phen)$_3$](ClO$_4$)$_3$·2H$_2$O, was prepared according to standard procedures,[9] and the purity was confirmed by elemental analysis and its UV–vis spectrum.[10]

The presence of H$_2$O caused complications (see Discussion). Recrystallization of [Co(*o*-phen)$_3$](ClO$_4$)$_3$·2H$_2$O from CH$_3$CN by slow addition of Et$_2$O produced an anhydrous product that showed none of the difficulties of the aquo complexes. We have also removed the ClO$_4^-$ by reaction of a suspension of [Co(*o*-phen)$_3$](ClO$_4$)$_3$·2H$_2$O with a saturated aqueous solution of KPF$_6$. Stirring for 2 days and filtering and then repeating the process led to complete exchange of ClO$_4^-$ by PF$_6^-$, as shown by the infrared stretches at 820 cm^{-1} for the PF$_6^-$ salt and 1050 and 600 cm^{-1} for the ClO$_4^-$ salt. The PF$_6^-$ salt [Co(*o*-phen)$_3$](PF$_6$)$_3$·xH$_2$O was recrystallized from CH$_3$CN/Et$_2$O in an inert-atmosphere glovebox to remove the water of hydration.

3-Acetoxy-*N*-methylpyridinium tetrafluoroborate was prepared from a slight excess of [Me$_3$O][BF$_4$] (3.25 g, 0.022 mmol) in de-

† University of California, Irvine.

(1) Meyer, T. J. *Prog. Inorg. Chem.* **1983**, *36*, 389.
(2) Taube, H.; Gould, E. S. *Acc. Chem. Res.* **1969**, *2*, 1225.
(3) Marcus, R. A. *Ann. Rev. Phys. Chem.* **1964**, *15*, 155.
(4) (a) Eyler, J. R.; Richardson, D. E. *J. Am. Chem. Soc.* **1985**, *107*, 6130. (b) Haaland, A. *Acc. Chem. Res.* **1979**, *12*, 415.
(5) (a) Braddock, J. N.; Meyer, T. J. *Inorg. Chem.* **1973**, *12*, 723. (b) Schmidt, S. P.; Trogler, W. C.; Basolo, F. *J. Am. Chem. Soc.* **1984**, *106*, 1308.
(6) (a) Zhen, Y.; Atwood, J. D. *J. Am. Chem. Soc.* **1989**, *111*, 1506. (b) Corraine, M. S.; Atwood, J. D. *Inorg. Chem.* **1989**, *28*, 3781. (c) Corraine, M. S.; Atwood, J. D. *Organometallics* **1991**, *10*, 2315. (d) Corraine, M. S.; Atwood, J. D. *Organometallics* **1991**, *10*, 2647. (e) Zhen, Y. Q.; Feighery, W. G.; Lai, C. K.; Atwood, J. D. *J. Am. Chem. Soc.* **1989**, *111*, 7832. (f) Zhen, Y.; Atwood, J. D. *Organometallics* **1991**, *10*, 2778. (g) Zhen, Y.; Feighery, W. G.; Atwood, J. D. *J. Am. Chem. Soc.* **1991**, *113*, 3616.
(7) Lai, C. K.; Feighery, W. G.; Zhen, Y.; Atwood, J. D. *Inorg. Chem.* **1989**, *28*, 3929.
(8) Beck, W.; Hieber, W.; Braun, G. *Z. Anorg. Allg. Chem.* **1961**, *308*, 23.
(9) (a) Przystas, T. J.; Sutin, N. *J. Am. Chem. Soc.* **1973**, *95*, 5545. (b) Schilt, A. A.; Taylor, R. C. *J. Inorg. Nucl. Chem.* **1959**, *9*, 211.
(10) Zahir, K.; Espenson, J.; Bakac, A. *Inorg. Chem.* **1988**, *27*, 3144.

0276-7333/92/2311-0035$03.00/0

gassed acetone (20 mL) added dropwise at room temperature to an acetone solution of 3-acetoxypyridine (2.74 g, 0.02 mmol). The resulting mixture was stirred overnight under Ar and filtered. The solvent was removed in vacuum and the white product recrystallized twice from either THF/pentane or CH_3CN/ether.

Reactions between Metal Carbonyl Anions and Co(III) Complexes. For each reaction an excess of Co(III) complex and metal carbonyl anion were mixed in 15 mL of CH_3CN. An infrared spectrum was recorded immediately, and the reaction was monitored by infrared spectroscopy until complete. The solvent was removed, and the residue was extracted with hexanes, separated by column chromatography and characterized by infrared spectroscopy showing formation of the metal carbonyl dimers, M_2. The spectral data of the dimers are shown in Table S1, supplementary material. The remaining solid was dissolved in CH_3CN and characterized by IR and UV–vis spectroscopy.

Kinetic Studies. All the kinetic experiments were performed on an IR stopped-flow spectrophotometer as described previously.[6b] All reactions were performed under pseudo-first-order conditions with at least a 10-fold excess of cobalt(III) complex at 25 °C. Typical concentrations of metal carbonyl anion and Co(III) for the kinetic studies were 0.001 and 0.10–0.30 M in CH_3CN depending on the reaction rates. The rates were monitored by the decrease in intensity of the infrared absorbance in CH_3CN at 1784, 1860, 1860, 1886, 1780, 1795, 1790, and 1806 cm^{-1} for anions $CpFe(CO)_2^-$, $Re(CO)_5^-$, $Mn(CO)_5^-$, $Co(CO)_4^-$, $CpMo(CO)_3^-$, $Mn(CO)_4(PBu_3)^-$, $Mn(CO)_4(PEt_3)^-$, and $Mn(CO)_4(PPh_3)^-$, respectively. The observed rate constants, the standard deviation, and the error at the chosen confidence limit were calculated using the OLIS stopped-flow operating system. Error limits in the second-order rate constants are quoted at 95% confidence limits.

The effect of added electrolyte was examined for several reactions of [PPN][$Re(CO)_5$]. These reactions are accomplished just as described above for the kinetics except that a salt (usually [NBu_4][BF_4]) is added to the cobalt solution in known quantities. The kinetics are then evaluated.

Collection of X-ray Diffraction Data for [PPN^+][$Mn(CO)_5^-$]. A yellow crystal of approximate dimensions 0.20 × 0.39 × 0.40 mm was sealed into a thin-walled capillary. It was then mounted and accurately aligned on the Syntex $P2_1$ automated four-circle diffractometer at the University at Buffalo–SUNY. The determination of Laue symmetry, crystal class, unit cell parameters, and the crystal's orientation matrix was carried out by previously described techniques.[11] Room-temperature (23 °C) intensity data were collected using the θ–2θ scan technique with Mo K$\bar{\alpha}$ radiation under the conditions given in Table I. All 5119 data were corrected for absorption and for Lorentz and polarization effects and placed on an approximately absolute scale by means of a Wilson plot. A careful survey of a preliminary data set revealed no systematic extinctions nor any diffraction symmetry other than the Friedel condition. Possible space groups are the noncentrosymmetric triclinic $P1$ [C_1^1; No. 1] or the centrosymmetric $P\bar{1}$ [C_i^1; No. 2]. The centrosymmetric space group was selected on the basis of intensity statistics and later confirmed as the correct choice by successful solution and refinement of the structure.

Solution and Refinement of the Crystal Structure of [PPN^+][$Mn(CO)_5^-$]. All crystallographic calculations were carried out using either the UCI-modified version of the UCLA Crystallographic Computing Package[12] or the SHELXTL PLUS program set.[13] The analytical scattering factors for neutral atoms were used throughout the analysis;[14a] both the real ($\Delta f'$) and imaginary ($i\Delta f''$) components of anomalous dispersion[14b] were included. The quantity minimized during least-squares analysis was $\Sigma w(|F_o| - |F_c|)^2$.

The positions of the manganese and two phosphorus atoms were determined from an automatic Patterson calculation (SHELXTL PLUS). The remaining nonhydrogen atoms were located from a series of difference-Fourier syntheses. Hydrogen atom contributions were included using a riding model with d(C–H) = 0.96 Å and U(iso) = 0.08 Å^2. Full-matrix least-squares refinement of positional and thermal parameters led to convergence with R_F = 6.2%, R_{wF} = 6.1%, and GOF = 1.01 for 451 variables refined against all 4374 unique data, (R_F = 3.7%, R_{wF} = 4.9% for those 3088 data with $|F_o| > 6.0\sigma(|F_o|)$). A final difference-Fourier synthesis showed no significant features (ρ(max) = 0.30 e Å^{-3} at a distance of 1.00 Å from O(5)). Final positional parameters are listed in Table II.

Table I. Experimental Data for the X-ray Diffraction Studies of [PPN^+][$Mn(CO)_5^-$] and [PPN^+][$Mn(CO)_4(PEt_3)^-$]·THF

	[PPN^+][$Mn(CO)_5^-$]	[PPN^+][$Mn(CO)_4(PEt_3^-)$]·THF
	(A) Crystal Data	
cryst syst	triclinic	triclinic
space group	$P\bar{1}$ (No. 2)	$P\bar{1}$ (No. 2)
a, Å	11.339 (2)	9.216 (2)
b, Å	11.579 (2)	14.059 (3)
c, Å	14.540 (3)	18.418 (5)
α, deg	77.030 (12)	96.875 (19)
β, deg	77.553 (13)	93.274 (18)
γ, deg	89.530 (13)	94.497 (17)
V, Å^3	1814.9 (5)	2356.7 (9)
Z	2	2
formula	$C_{41}H_{30}MnNO_5P_2$	$C_{50}H_{53}MnNO_5P_3$
fw	733.5	895.8
D(calcd), g/cm^3	1.34	1.26
μ, mm^{-1}	0.48	0.41

(B) Data Collection

diffractometer: Syntex $P2_1$
radiation: Mo K$\bar{\alpha}$ ($\bar{\lambda}$, 0.71073 Å)
monochromator: pyrolytic graphite, equatorial mode, assumed 50% perfect
scan conditions: coupled θ(crystal)–2θ(counter), at 4.0 deg/min (2θ) from [$2\theta(K\alpha_1)$ – 1.0]° to [$2\theta(K\alpha_2)$ + 1.0]°; 2θ range 4.5–45.0°; one hemisphere ($+h,\pm k,\pm l$) collected
no. of reflections collected: 5119, yielding 4374 unique data with $|F_o| > 0$ for [PPN^+][$Mn(CO)_5^-$]; 6660, yielding 5705 with $|F_o| > 0$ and 4790 with $|F_o| > 3\sigma$ (used in the analysis) for [PPN^+][$Mn(CO)_4(PEt_3)^-$]·THF

Collection of X-ray Diffraction Data for [PPN^+][$Mn(CO)_4(PEt_3)^-$]·THF. A red-orange crystal of approximate dimensions 0.20 × 0.30 × 0.70 mm was inserted into a thin-walled glass capillary under an inert (Ar) atmosphere. It was then mounted and accurately aligned on the Syntex $P2_1$ automated four-circle diffractometer as described above. The determination of Laue symmetry, crystal class, unit cell parameters, and the crystal's orientation matrix was carried out by previously described techniques.[11] Room-temperature (23 °C) intensity data were collected using the θ–2θ scan technique with Mo K$\bar{\alpha}$ radiation under the conditions given in Table I. All 6660 data were corrected for absorption and for Lorentz and polarization effects. Any reflection with I(net) < 0 was assigned the value $|F_o| = 0$. A careful survey of a preliminary data set revealed no systematic extinctions nor any diffraction symmetry other than the Friedel condition. Possible space groups are the noncentrosymmetric triclinic $P1$ [C_1^1; No. 1] or the centrosymmetric $P\bar{1}$ [C_i^1; No. 2]. The centrosymmetric space group was chosen and later confirmed as the correct choice by successful solution and refinement of the structure.

Solution and Refinement of the Crystal Structure of [PPN^+][$Mn(CO)_4PEt_3^-$]·THF. All crystallographic calculations were carried out using either the UCI-modified version of the UCLA Crystallographic Computing Package[12] or the SHELXTL PLUS program set.[13] The analytical scattering factors for neutral atoms were used throughout the analysis;[14a] both the real ($\Delta f'$) and imaginary ($i\Delta f''$) components of anomalous dispersion[14b] were included. The quantity minimized during least-squares analysis was $\Sigma w(|F_o| - |F_c|)^2$.

The positions of the manganese and three phosphorus atoms were determined from an "E map" (SHELXTL PLUS). The remaining

(11) Churchill, M. R.; Lashewycz, R. A.; Rotella, F. J. *Inorg. Chem.* **1977**, *16*, 265.
(12) *UCLA Crystallographic Computing Package*; University of California; Los Angeles, 1981 C. Strouse, personal communication.
(13) Nicolet Instrument Corp., Madison, WI, 1988.
(14) *International Tables for X-Ray Crystallography*; Kynoch Press: Birmingham, England, 1974; (a) pp 99–101, (b) pp 149–150.

Table II. Final Atomic Coordinates (×10^4) and Equivalent Isotropic Thermal Parameters (Å^2 × 10^3) for [PPN$^+$][Mn(CO)$_5^-$]

	x	y	z	U(eq)[a]
Mn(1)	1471.9 (0.5)	1770.0 (0.5)	2412.4 (0.4)	40.8 (0.3)
P(1)	4203.2 (0.9)	3180.4 (0.8)	7905.1 (0.7)	32.0 (0.4)
P(2)	6594.8 (0.9)	3528.8 (0.9)	6493.8 (0.7)	33.7 (0.4)
O(1)	−24 (3)	−403 (3)	3488 (3)	75 (2)
O(2)	145 (3)	3212 (3)	3706 (3)	80 (2)
O(3)	2921 (4)	3919 (3)	1281 (3)	96 (2)
O(4)	3692 (3)	746 (3)	2945 (3)	85 (2)
O(5)	763 (4)	1580 (4)	613 (3)	104 (2)
N(1)	5220 (3)	3608 (3)	6968 (2)	40 (1)
C(1)	560 (4)	441 (4)	3069 (3)	51 (2)
C(2)	650 (4)	2632 (4)	3207 (3)	52 (2)
C(3)	2365 (4)	3075 (4)	1734 (3)	55 (2)
C(4)	2812 (4)	1123 (4)	2739 (3)	55 (2)
C(5)	1036 (4)	1639 (4)	1326 (4)	59 (2)
C(6)	4733 (3)	2840 (3)	9009 (3)	33 (1)
C(7)	4495 (4)	1750 (3)	9664 (3)	45 (2)
C(8)	4949 (5)	1552 (4)	10488 (3)	59 (2)
C(9)	5636 (5)	2417 (4)	10661 (3)	62 (2)
C(10)	5874 (4)	3497 (4)	10022 (3)	54 (2)
C(11)	5422 (4)	3711 (3)	9199 (3)	42 (2)
C(12)	3165 (3)	4350 (3)	8018 (3)	36 (1)
C(13)	3075 (4)	5210 (4)	7208 (4)	61 (2)
C(14)	2267 (5)	6097 (5)	7308 (5)	85 (3)
C(15)	1573 (5)	6142 (5)	8172 (5)	77 (3)
C(16)	1663 (4)	5292 (5)	8980 (4)	66 (2)
C(17)	2459 (4)	4395 (4)	8910 (3)	48 (2)
C(18)	3368 (3)	1875 (3)	7875 (3)	36 (1)
C(19)	3987 (4)	975 (3)	7537 (3)	39 (2)
C(20)	3377 (4)	−76 (3)	7574 (3)	46 (2)
C(21)	2161 (5)	−218 (4)	7943 (4)	63 (2)
C(22)	1544 (4)	678 (5)	8278 (5)	84 (3)
C(23)	2135 (4)	1736 (4)	8240 (4)	63 (2)
C(24)	7544 (3)	3115 (3)	7350 (3)	37 (1)
C(25)	7442 (4)	1971 (4)	7920 (3)	49 (2)
C(26)	8079 (5)	1676 (5)	8647 (3)	64 (2)
C(27)	8838 (5)	2502 (6)	8791 (4)	71 (2)
C(28)	8953 (4)	3629 (5)	8214 (4)	70 (2)
C(29)	8324 (4)	3941 (4)	7492 (3)	52 (2)
C(30)	7146 (3)	4951 (3)	5730 (3)	39 (2)
C(31)	8097 (5)	5048 (4)	4938 (3)	64 (2)
C(32)	8508 (5)	6147 (5)	4374 (4)	85 (3)
C(33)	8010 (6)	7152 (5)	4595 (4)	80 (3)
C(34)	7098 (5)	7072 (4)	5380 (4)	67 (2)
C(35)	6646 (4)	5972 (4)	5958 (3)	54 (2)
C(36)	6795 (4)	2467 (3)	5743 (3)	39 (2)
C(37)	7865 (4)	1874 (3)	5586 (3)	48 (2)
C(38)	7989 (5)	1057 (4)	5020 (3)	60 (2)
C(39)	7060 (6)	831 (4)	4607 (3)	70 (2)
C(40)	6009 (5)	1416 (5)	4748 (3)	68 (2)
C(41)	5869 (4)	2242 (4)	5317 (3)	52 (2)

[a] Equivalent isotropic U defined as one-third of the trace of the orthogonalized U_{ij} tensor.

non-hydrogen atoms were located from a series of difference-Fourier syntheses. The α-carbon atoms of the triethylphosphine ligand are disordered. Hydrogen atom contributions were included using a riding model with d(C–H) = 0.96 Å[15] and U(iso) = 0.08 Å^2. Hydrogen atoms associated with the disordered atoms were not included. An unsuspected THF molecule of solvation was also found. Full-matrix least-squared refinement of positional and thermal parameters led to convergence with R_F = 6.1%, R_{wF} = 7.4%, and GOF = 1.59 for 568 variables refined against those 4790 unique data with $|F_o| > 3.0\sigma(|F_o|)$, (R_F = 5.1%, R_{wF} = 6.8% for those of 4101 data with $|F_o| > 6.0\sigma(|F_o|)$). A final difference–Fourier synthesis showed no significant features (ρ(max) = 0.39 e Å^{-3} at a distance of 1.24 Å from C(7B)). Final positional parameters are listed in Table III.

Results and Discussion

All the reactions reported in this manuscript have rate laws that are first order in oxidant and first order in reductant.

$$\text{rate} = k[\text{metal carbonyl anion}][\text{oxidant}]$$

The rate constants are obtained from plots of the pseudo-first-order rate constants, k_{obs}, versus [oxidant]. Rate constants for the reaction of [Co(*o*-phen)$_3$][PF$_6$]$_3$, [Co(*o*-phen)$_3$][ClO$_4$]$_3$, and 3-acetoxy-*N*-methylpyridinium tetra-

(15) Churchill, M. R. *Inorg. Chem.* **1973**, *12*, 1213.

Table III. Final Atomic Coordinates (×10^4) and Equivalent Isotropic Thermal Parameters (Å^2 × 10^3) for [PPN$^+$][Mn(CO)$_4$(PEt$_3$)$^-$]•THF

	x	y	z	U(eq)[a]
Mn(1)	3906.5 (0.8)	3312.8 (0.5)	7339.7 (0.4)	52.4 (0.3)
P(1)	5317 (2)	4319 (1)	6771 (1)	76 (1)
O(1)	5131 (5)	1590 (3)	6644 (2)	101 (2)
O(2)	1983 (6)	2091 (3)	8116 (3)	121 (2)
O(3)	5372 (6)	4227 (3)	8745 (2)	105 (2)
O(4)	1384 (5)	4026 (3)	6586 (3)	102 (2)
C(1)	4660 (7)	2296 (4)	6908 (3)	71 (2)
C(2)	2734 (7)	2571 (4)	7807 (3)	72 (2)
C(3)	4784 (6)	3872 (4)	8188 (3)	68 (2)
C(4)	2395 (7)	3747 (4)	6890 (3)	66 (2)
C(5A)	5745 (19)	5577 (11)	7240 (10)	101 (7)
C(5B)	4653 (17)	5567 (7)	6721 (7)	92 (6)
C(6)	4280 (10)	6052 (5)	7437 (4)	110 (4)
C(7A)	4647 (35)	4570 (16)	5850 (10)	111 (12)
C(7B)	5572 (19)	3946 (12)	5766 (8)	127 (7)
C(8)	4222 (15)	3668 (6)	5318 (5)	155 (2)
C(9A)	7177 (16)	4683 (14)	7165 (12)	139 (9)
C(9B)	7380 (30)	3933 (19)	6699 (17)	152 (14)
C(10)	8057 (13)	3774 (12)	7274 (9)	194 (8)
P(2)	1410 (1)	822 (1)	11674 (1)	42 (1)
P(3)	1877 (1)	1285 (1)	13299 (1)	42 (1)
N(1)	2088 (4)	1281 (3)	12456 (2)	50 (1)
C(11)	2297 (5)	1491 (3)	11023 (2)	45 (2)
C(12)	2717 (6)	2456 (4)	11212 (3)	66 (2)
C(13)	3410 (7)	2975 (4)	10727 (4)	82 (3)
C(14)	3677 (7)	2543 (5)	10053 (3)	83 (3)
C(15)	3279 (7)	1594 (5)	9862 (3)	84 (3)
C(16)	2586 (6)	1049 (4)	10342 (3)	64 (2)
C(17)	1766 (5)	−410 (3)	11453 (2)	43 (2)
C(18)	827 (6)	−1047 (4)	10986 (3)	64 (2)
C(19)	1177 (8)	−1979 (4)	10797 (3)	84 (3)
C(20)	2459 (9)	−2262 (5)	11076 (4)	87 (3)
C(21)	3383 (7)	−1632 (5)	11540 (3)	81 (3)
C(22)	3039 (6)	−718 (4)	11730 (3)	61 (2)
C(23)	−528 (5)	895 (3)	11546 (3)	50 (2)
C(24)	−1454 (6)	298 (4)	11889 (3)	59 (2)
C(25)	−2932 (7)	383 (5)	11845 (3)	82 (3)
C(26)	−3476 (7)	1060 (6)	11457 (4)	98 (3)
C(27)	−2585 (7)	1637 (5)	11118 (4)	102 (3)
C(28)	−1108 (6)	1570 (4)	11161 (3)	74 (2)
C(29)	992 (5)	2327 (3)	13645 (3)	49 (2)
C(30)	888 (8)	2561 (4)	14385 (3)	86 (3)
C(31)	193 (8)	3348 (5)	14649 (4)	106 (3)
C(32)	−396 (7)	3908 (4)	14160 (4)	90 (3)
C(33)	−309 (7)	3685 (4)	13427 (4)	83 (3)
C(34)	378 (6)	2895 (4)	13172 (3)	62 (2)
C(35)	857 (5)	258 (3)	13561 (2)	47 (2)
C(36)	−571 (6)	302 (4)	13736 (3)	71 (2)
C(37)	−1400 (7)	−537 (6)	13859 (3)	96 (3)
C(38)	−816 (11)	−1386 (5)	13824 (4)	99 (4)
C(39)	585 (11)	−1434 (4)	13660 (4)	101 (4)
C(40)	1466 (7)	−619 (4)	13523 (3)	70 (2)
C(41)	3644 (5)	1367 (3)	13769 (2)	44 (2)
C(42)	3868 (6)	1106 (4)	14469 (3)	57 (2)
C(43)	5217 (7)	1224 (4)	14830 (3)	70 (2)
C(44)	6370 (7)	1599 (5)	14506 (4)	85 (3)
C(45)	6209 (7)	1863 (5)	13803 (4)	84 (3)
C(46)	4830 (6)	1738 (4)	13435 (3)	61 (2)
O(5)	−1267 (17)	3843 (6)	10671 (7)	224 (7)
C(47)	−481 (18)	4341 (11)	11230 (8)	219 (10)
C(48)	−565 (17)	5269 (13)	11232 (9)	224 (11)
C(49)	−1617 (20)	5407 (9)	10731 (9)	194 (9)
C(50)	−2299 (14)	4486 (15)	10519 (8)	236 (10)

[a] Equivalent isotropic U defined as one-third of the trace of the orthogonalized U_{ij} tensor.

Table IV. Second-Order Rate Constants for the Reaction of Metal Carbonyl Anions with $[Co(o\text{-phen})_3][X]_3$ in CH_3CN

anion	X	k, s^{-1} M^{-1}
$CpFe(CO)_2^-$	PF_6^-	5400 ± 1700
$Re(CO)_5^-$	PF_6^-	4000 ± 1000
$Mn(CO)_5^-$	PF_6^-	2000 ± 100
$CpMo(CO)_3^-$	PF_6^-	1900 ± 400
$CpFe(CO)_2^-$	ClO_4^-	1800 ± 700
$Re(CO)_5^-$	ClO_4^-	1500 ± 600
$Mn(CO)_5^-$	ClO_4^-	1100 ± 400
$CpMo(CO)_3^-$	ClO_4^-	800 ± 300
$Mn(CO)_4PEt_3^-$	ClO_4^-	230 ± 60
$Mn(CO)_4PBu_3^-$	ClO_4^-	220 ± 40
$Mn(CO)_4PPh_3^-$	ClO_4^-	190 ± 40

Table V. Rate Constants for the Reaction between Metal Carbonyl Anions and 3-Acetoxy-*N*-methylpyridinium tetrafluoroborate in CH_3CN at 25 °C

	k, s^{-1} M^{-1}		k, s^{-1} M^{-1}
$[PPN][CpFe(CO)_2]$	1180 ± 40	$[PPN][Mn(CO)_5]$	31 ± 2
$[PPN][Re(CO)_5]$	113 ± 7	$[PPN][Co(CO)_4]$	0.22 ± 0.01
$[PPN][CpMo(CO)_3]$	69 ± 1	$[Na][Re(CO)_5]$	14.4 ± 0.2

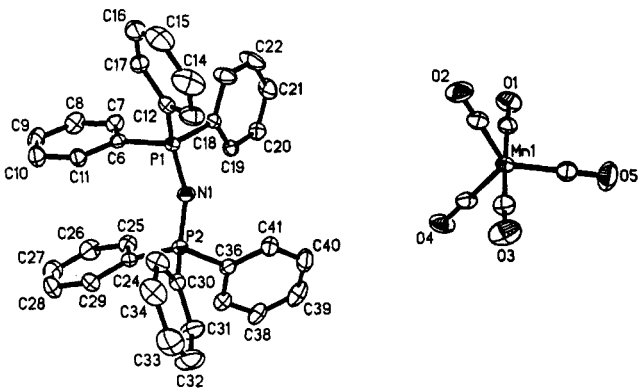

Figure 1. ORTEP diagram for $[PPN^+][Mn(CO)_5^-]$.

fluoroborate with various metal carbonyl anions are given in Tables IV and V. Reactions of anions with $[Fe(o\text{-phen})_3][ClO_4]_3$ were too rapid for examination by our stopped-flow system.

Each of these oxidants are known to react by outer-sphere electron transfer.[16-20] $Fe(o\text{-phen})_3^{3+}$ reacts more rapidly than $Co(o\text{-phen})_3^{3+}$. This is consistent with the known order of outer-sphere electron-transfer reactivity.[16,17] To aid in the interpretation of possible intrinsic barriers to outer-sphere reactions, we have determined the structures of $Mn(CO)_4L^-$, L = CO, PEt_3.

Crystal Structure of $[PPN^+][Mn(CO)_5^-]$. The structure (see Figure 1) consists of discrete PPN^+ cations and $Mn(CO)_5^-$ anions, separated at normal van der Waals' distances. Interatomic distances and angles are collected in Table VI.

The $Mn(CO)_5^-$ anion has a slightly distorted trigonal-bipyramidal structure. The diaxial angle is C(1)–Mn(1)–C(3) = 178.4 (2)°, and the two axial Mn–CO bond lengths are Mn(1)–C(1) = 1.814 (4) Å and Mn(1)–C(3) = 1.791 (4) Å (average axial Mn–CO distance is 1.803 Å). The equatorial Mn–CO distances are Mn(1)–C(2) = 1.799 (5) Å, Mn(1)–C(4) = 1.797 (5) Å, and Mn–C(5) = 1.791 (6) Å (average = 1.796 Å). One surprising feature is an irregularity in the diequatorial OC–Mn–CO angles with one small angle, C(2)–Mn(1)–C(4) = 115.7 (2)°, and two large angles, C(2)–Mn(1)–C(5) = 122.2 (2)° and C(4)–Mn(1)–C(5) = 122.0 (2)°.

Table VI. Important Bond Lengths (Å) and Angles (deg) for $[PPN^+][Mn(CO)_5^-]$

(A) Distances within the $[Mn(CO)_5^-]$ Anion

Mn(1)–C(1)	1.814 (4)	Mn(1)–C(2)	1.799 (5)
Mn(1)–C(3)	1.791 (4)	Mn(1)–C(4)	1.797 (5)
Mn(1)–C(5)	1.791 (6)	O(1)–C(1)	1.155 (5)
O(2)–C(2)	1.157 (6)	O(3)–C(3)	1.153 (5)
O(4)–C(4)	1.157 (6)	O(5)–C(5)	1.160 (7)

(B) OC–Mn–CO Angles

C(1)–Mn(1)–C(2)	91.8 (2)	C(1)–Mn(1)–C(3)	178.4 (2)
C(2)–Mn(1)–C(3)	89.3 (2)	C(1)–Mn(1)–C(4)	91.7 (2)
C(2)–Mn(1)–C(4)	115.7 (2)	C(3)–Mn(1)–C(4)	89.0 (2)
C(1)–Mn(1)–C(5)	89.8 (2)	C(2)–Mn(1)–C(5)	122.2 (2)
C(3)–Mn(1)–C(5)	88.6 (2)	C(4)–Mn(1)–C(5)	122.0 (2)

(C) Mn–C–O Angles

Mn(1)–C(1)–O(1)	179.7 (5)	Mn(1)–C(2)–O(2)	178.1 (4)
Mn(1)–C(3)–O(3)	178.3 (5)	Mn(1)–C(4)–O(4)	177.7 (4)
Mn(1)–C(5)–O(5)	178.5 (4)		

(D) P–N Distances and P–N–P Angle in the $[PPN^+]$ Cation

P(1)–N(1)	1.569 (3)	P(1)–N(1)–P(2)	144.9 (2)
P(2)–N(1)	1.573 (3)		

(E) P–C Distances

P(1)–C(6)	1.795 (4)	P(2)–C(24)	1.800 (4)
P(1)–C(12)	1.800 (4)	P(2)–C(30)	1.798 (4)
P(1)–C(18)	1.804 (4)	P(2)–C(36)	1.802 (4)

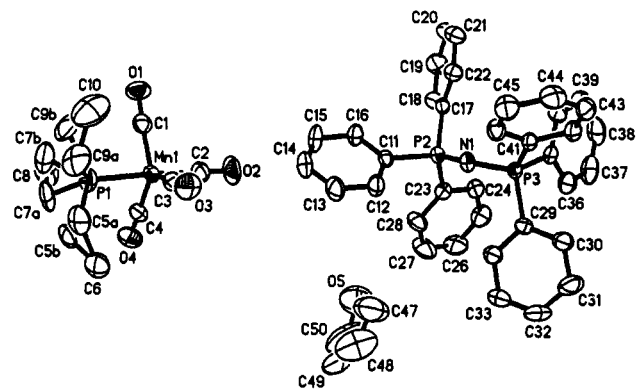

Figure 2. ORTEP diagram for $[PPN^+][Mn(CO)_4(PEt_3)^-]\cdot THF$. Note the disorder of the α-carbons of the PEt_3 ligand.

Parameters obtained in this study are consistent with, but more accurate than, those obtained by Frenz and Ibers for $[Ni(1,10\text{-phenanthroline})_3^{2+}][Mn(CO)_5^-]_2$ in which (for two independent $Mn(CO)_5^-$ anions) Mn–CO(axial) = 1.802 (11)–1.832 (11) Å (average = 1.820 ± 0.014 Å), Mn–CO(equatorial) = 1.772 (11)–1.818 (12) Å (average = 1.798 (15) Å), and <OC–Mn–CO(diaxial) = 178.2 (3)–178.6 (3)° (average – 178.4°).[21] In this structural study the equatorial $Mn(CO)_3$ fragment is again distorted from D_{3h} symmetry; however, the diequatorial angles are composed of two small and one large angles (117.5 (3), 117.6 (4), 125.0 (4)° in one anion; 118.0 (4), 118.5 (3), 123.4 (3)° in the other).

In each case the average Mn–CO(axial) distances are numerically larger than the average Mn–CO(equatorial) distances—by 0.007 Å for $[PPN^+][Mn(CO)_5^-]$ and by 0.022 Å for $[Ni(o\text{-phen})_3^{2+}][Mn(CO)_5^-]_2$—but in neither case is the difference *statistically* meaningful.

Crystal Structure of $[PPN^+][Mn(CO)_4(PEt_3)^-]\cdot THF$. The structure (see Figure 2) consists of equal quantities of PPN^+ cations, $Mn(CO)_4(PEt_3)^-$ anions, and

(16) Atwood, J. D. *Inorganic and Organometallic Reaction Mechanisms*; Brooks/Cole: Monterey, CA, 1985.
(17) Basolo, F.; Pearson, R. G. *Mechanisms of Inorganic Reactions*; John Wiley and Sons: New York, 1967.
(18) Dulz, G.; Sutin, N. *Inorg. Chem.* **1963**, *2*, 917.
(19) Ellis, P.; Wilkins, R. G.; Williams, M. J. G. *J. Chem. Soc.* **1957**, 4456.
(20) Burke, M. R.; Brown, T. L. *J. Am. Chem. Soc.* **1989**, *111*, 5185.
(21) Frenz, B. A.; Ibers, J. A. *Inorg. Chem.* **1972**, *11*, 1109.

Table VII. Important Bond Lengths (Å) and Angles (deg) for [PPN$^+$][Mn(CO)$_4$(PEt$_3$)$^-$]·THF

(A) Distances within the Mn(CO)$_4$P Moiety

Mn(1)–P(1)	2.239 (2)	Mn(1)–C(1)	1.762 (6)
Mn(1)–C(2)	1.772 (6)	Mn(1)–C(3)	1.782 (6)
Mn(1)–C(4)	1.768 (6)	O(1)–C(1)	1.177 (8)
O(2)–C(2)	1.151 (8)	O(3)–C(3)	1.169 (7)
O(4)–C(4)	1.176 (8)		

(B) Distances within the Disordered PEt$_3$ Ligand

P(1)–C(5A)	1.876 (15)	P(1)–C(5B)	1.913 (12)
P(1)–C(7A)	1.854 (21)	P(1)–C(7B)	1.894 (15)
P(1)–C(9A)	1.832 (15)	P(1)–C(9B)	2.025 (28)
C(5A)···C(5B)	1.346 (23)	C(5A)–C(6)	1.593 (20)
C(5B)–C(6)	1.482 (15)	C(7A)···C(7B)	1.272 (33)
C(7A)–C(8)	1.517 (21)	C(7B)–C(8)	1.454 (19)
C(9A)···C(9B)	1.310 (34)	C(9A)–C(10)	1.592 (26)
C(9B)–C(10)	1.249 (34)		

(C) Angles around Mn in the Mn(CO)$_4$P Moiety

P(1)–Mn(1)–C(1)	92.3 (2)	P(1)–Mn(1)–C(2)	176.8 (2)
C(1)–Mn(1)–C(2)	90.8 (3)	P(1)–Mn(1)–C(3)	88.3 (2)
C(1)–Mn(1)–C(3)	117.3 (3)	C(2)–Mn(1)–C(3)	90.8 (3)
P(1)–Mn(1)–C(4)	87.0 (2)	C(1)–Mn(1)–C(4)	118.5 (3)
C(2)–Mn(1)–C(4)	91.0 (3)	C(3)–Mn(1)–C(4)	124.1 (3)

(D) Mn–C–O Angles

Mn(1)–C(1)–O(1)	176.7 (5)	Mn(1)–C(2)–O(2)	179.3 (6)
Mn(1)–C(3)–O(3)	178.9 (6)	Mn(1)–C(4)–O(4)	179.3 (4)

(E) Mn–P–C(α) Angles

Mn(1)–P(1)–C(5A)	117.2 (6)	Mn(1)–P(1)–C(5B)	115.9 (5)
Mn(1)–P(1)–C(7A)	117.6 (9)	Mn(1)–P(1)–C(7B)	117.1 (5)
Mn(1)–P(1)–C(9A)	118.2 (7)	Mn(1)–P(1)–C(9B)	112.9 (8)

(F) P–N Distances and P–N–P Angles in the [PPN$^+$] Cation

P(2)–N(1)	1.579 (4)	P(2)–N(1)–P(3)	142.3 (3)
P(3)–N(1)	1.577 (4)		

(G) P–C Distances within the [PPN$^+$] Cation

P(2)–C(11)	1.802 (5)	P(3)–C(29)	1.800 (5)
P(2)–C(17)	1.791 (5)	P(3)–C(35)	1.791 (5)
P(2)–C(23)	1.800 (5)	P(3)–C(41)	1.789 (5)

THF (C_4H_8O) molecules of solvation. Interatomic distances and angles are collected in Table VII. The structural study is complicated by disorder within the PEt$_3$ ligand such that there are two sites for the α-carbon atoms (45% occupancy for the "A" atoms and 55% occupancy for the "B" atoms) and a common site for the β-carbon atoms of the two opposed rotomers.

The Mn(CO)$_4$(PEt$_3$)$^-$ anion again has a slightly distorted trigonal-bipyramidal structure, with the PEt$_3$ ligand in an axial site and a diaxial angle of P(1)–Mn(1)–C(2) = 176.8 (2)°. The axial Mn(1)–C(2) distance of 1.772 (6) Å may be compared with the equatorial bond lengths Mn(1)–C(1) = 1.762 (6) Å, Mn(1)–C(3) = 1.782 (6) Å, and Mn(1)–C(4) = 1.768 (6) Å (average = 1.770 Å). Once again the diequatorial angles are irregular, with C(3)–Mn(1)–C(4) = 124.1 (3)° as compared to C(1)–Mn(1)–C(3) = 117.3 (3)° and C(1)–Mn(1)–C(4) = 118.5 (3)°.

The most interesting comparison between the Mn(CO)$_5^-$ anion in [PPN$^+$][Mn(CO)$_5^-$] and the Mn(CO)$_4$(PEt$_3$)$^-$ anion in [PPN$^+$][Mn(CO)$_4$(PEt$_3$)$^-$] is that all of the Mn–CO bonds in the Mn(CO)$_4$(PEt$_3$)$^-$ anion are *shorter* (i.e., 1.762 (6)–1.782 (6) Å, average = 1.771 Å) than all of the Mn–CO bonds in the Mn(CO)$_5^-$ anion (i.e., 1.791 (6)–1.814 (4) Å, average = 1.798 Å). Thus, the structural effect of replacing one carbonyl ligand in Mn(CO)$_5^-$ with an axial PEt$_3$ ligand appears to be isotropic, rather than concentrated in the trans position. In the previously determined structure of Mn(CO)$_4$PPh$_3^-$, the axial and equatorial bonds were also the same length (1.796 (5) Å) and longer than for the L = PEt$_3$ complex.[22] It is interesting to note that the Mn–C bond length of Mn(CO)$_4$L$^-$ is shortened for L = PEt$_3$ relative to L = CO in a manner very similar to that observed for neutral complexes.

This shortening of the Mn–CO bonds of Mn(CO)$_4$L$^-$ for L = PEt$_3$ in comparison to L = PPh$_3$ or CO will lead to a larger intrinsic barrier to lengthen the Mn–CO bonds in formation of the activated complex for the PEt$_3$ complex. Such a barrier would partially offset the expected effect of the better donor PEt$_3$ on the potential. The kinetic studies of these complexes show very little difference in rate constant for reactions of Mn(CO)$_4$L$^-$ with Co(*o*-phen)$_3^{3+}$ as L is changed.

Mechanistic Considerations. Reaction of reducing agents with Co(*o*-phen)$_3^{3+}$ salts and with 3-acetoxy-*N*-methylpyridinium salts occur by outer-sphere electron transfer.[16-20] All of the data for reactions with the metal carbonyl anions are consistent with outer-sphere electron transfer. The much slower reactions of Co(*o*-phen)$_3^{3+}$ relative to Fe(*o*-phen)$_3^{3+}$ are anticipated for outer-sphere reactions. The dependence on the nature of the metal carbonyl anion is in the order expected from the driving force[23] for the reaction ($CpFe(CO)_2^-$ > $Re(CO)_5^-$ > $Mn(CO)_5^-$ ~ $CpMo(CO)_3^-$) although the rate changes with driving force are relatively minor for reaction with Co(*o*-phen)$_3^{3+}$. Phosphine-substituted manganese carbonyl ions show essentially no dependence on the nature of the phosphine; their reactions are somewhat slower than for $Mn(CO)_5^-$.

Aquated salts cannot be used for reaction with metal carbonyl anions. Interestingly, the reaction of metal carbonyl anions with H_2O in CH_3CN occurs ~3 orders of magnitude more *slowly* than reaction of the anions with Co(*o*-phen)$_3^{3+}$ and thus should not provide effective competition kinetically. However, reactions of metal carbonyl anions with [Co(*o*-phen)$_3$][ClO$_4$]$_3$·H_2O occur much more slowly than with the anhydrous salt and on the same time scale as reactions of the metal carbonyl anions with H_2O. We have not pursued this effect of H_2O in detail, but believe that solvation (possibly hydrogen-bonding) affects the reactions of the metal carbonyl anions.

Outer Sphere versus Nucleophilic Attack Mechanisms for Reactions of Metal Carbonyl Anions. We have now reported several reactions of metal carbonyl anions that occur by nucleophilic attack of the anion on the oxidant or by an outer-sphere (single-electron transfer) mechanism. The reactions that occur by nucleophilic attack have a much larger dependence on the *nature* of the metal carbonyl anion than do those that occur by outer-sphere electron transfer. For example, consider $Re(CO)_5^-$ and $CpMo(CO)_3^-$. These react via nucleophilic attack on CH_3I with relative rates of 200:1. In contrast to this, these same two metal carbonyl anions react via an outer-sphere electron-transfer mechanism with Co(*o*-phen)$_3^{3+}$ with relative rates of only 2:1 and with the 3-acetoxy-*N*-methylpyridinium ion with relative rates of again only 2:1. The effect of changing the counterion (i.e. use of $Na^+Re(CO)_5^-$ rather than $PPN^+Re(CO)_5^-$) is unpredictable.[25-27] In the reaction of MeI, this causes a *decrease* in rate by a factor of 2; in the reaction with $Cp_2Mo_2(CO)_6$, it causes a 4-fold rate *increase*; in the reaction with $Ru_3(CO)_{12}$ there is *no* detectable rate change; in the reaction with the 3-acetoxy-*N*-methylpyridinium ion,

(22) Riley, P. E.; Davis, R. E. *Inorg. Chem.* **1980**, *19*, 159.

(23) The potentials for oxidation of the metal carbonyl anions have been evaluated.[24]

(24) Tilset, M.; Parker, V. D. *J. Am. Chem. Soc.* **1989**, *111*, 6711.

(25) Darensbourg, M. Y. *Prog. Inorg. Chem.* **1985**, *33*, 221.

(26) Ungvary, F.; Wojcicki, A. *J. Am. Chem. Soc.* **1987**, *109*, 6848.

(27) Collman, J. P.; Finke, R. G.; Cawse, J. N.; Brauman, J. I. *J. Am. Chem. Soc.* **1978**, *100*, 4766.

it causes a 10-fold rate *decrease*; and in the reaction with $Co(o\text{-phen})_3^{3+}$, it causes a 2-fold rate *increase*.

In the reaction of M^- with $Co(o\text{-phen})_3^{3+}$ as reported in this manuscript, the concentration of ions is large ($\sim 10^{-2}$ M). To ascertain a possible effect of ionic strength, we have examined this reaction and a few other reactions in the presence of excess $[NBu_4][BF_4]$ (0.01 → 0.04 M). For reaction of $[PPN][Re(CO)_5^-]$ with $[Co(o\text{-phen})_3][PF_6]$, addition of $[NBu_4][BF_4]$ led to a small decrease in rate, $k_{obs} = 1.8 \pm 0.1\ s^{-1}$ for $[[NBu_4][BF_4]] = 0$ M, $k_{obs} = 1.4 \pm 0.2$ for $[[NBu_4][BF_4]] = 0.020$ M. A similar small decrease in rate is observed when 3-acetoxy-*N*-methylpyridinium is reacted with $Re(CO)_5^-$ in the presence of $[NBu_4][BF_4]$. Reaction of $Ru_3(CO)_{12}$ with $Re(CO)_5^-$ is slowed by a factor of 4 in the presence of excess salt. For none of these reactions are ionic effects a dominant factor in the overall reaction rate.

Conclusion. In this manuscript we have examined the outer-sphere electron-transfer reactions of a series of metal carbonyl anions with $Co(o\text{-phen})_3^{3+}$ and with 3-acetoxy-*N*-methylpyridinium. There exists only a small change in reactivity with the nature of the metal carbonyl anion. Structures of $Mn(CO)_5^-$ and $Mn(CO)_4PEt_3^-$ show that the expected increase in potential by the PEt_3 donor is offset by an increased intrinsic barrier due to shortening of the Mn–CO bonds for the PEt_3 complex. The effect of the Na^+ counterion is small and unpredictable for the reactions of metal carbonyl anions. The presence of a noninteracting salt causes a small decrease in the rate of reaction of $Re(CO)_5^-$ with $Co(o\text{-phen})_3^{3+}$ or with 3-acetoxy-*N*-methylpyridinium. The very small effect of the nature of the metal carbonyl anion is the most diagnostic feature for an outer-sphere reaction.

Acknowledgment. We acknowledge the Department of Energy (Grant ER 13775) for support of this research, and we thank William Feighery and Jerry Keister for helpful discussions.

Registry No. $[PPN^+][Mn(CO)_5^-]$, 137203-43-1; $[PPN^+][Mn(CO)_4(PEt_3)^-]\cdot THF$, 137428-92-3; $[PPN^+][CpFe(CO)_2^-]$, 122521-41-9; $[PPN^+][CpRe(CO)_5^-]$, 119207-87-3; $[PPN^+][CpMo(CO)_3^-]$, 67486-18-4; $[Co(o\text{-phen})_3][PF_6]_3$, 28277-59-0; $[Co(o\text{-phen})_3][ClO_4]_3$, 14516-66-6; $Fe(o\text{-phen})_3^{3+}$, 13479-49-7; $CpFe(CO)_2^-$, 12107-09-4; $Re(CO)_5^-$, 14971-38-1; $Mn(CO)_5^-$, 35816-56-9; $CpMo(CO)_3^-$, 12126-18-0; $Mn(CO)_4PEt_3^-$, 137328-86-0; $Mn(CO)_4PBu_3^-$, 122521-42-0; $Mn(CO)_4PPh_3^-$, 53418-18-1; $[PPN][Co(CO)_4]$, 53433-12-8; $[Na][Re(CO)_5]$, 33634-75-2; $Re_2(CO)_{10}$, 14285-68-8; $Mn_2(CO)_{10}$, 10170-69-1; $Co_2(CO)_8$, 10210-68-1; $Cp_2Fe_2(CO)_4$, 12154-95-9; $Cp_2Mo_2(CO)_6$, 12091-64-4; 3-acetoxy-*N*-methylpyridinium tetrafluoroborate, 121758-03-0.

Supplementary Material Available: For $[PPN^+][Mn(CO)_5^-]$, tables of microanalyses, infrared spectral data, sample rate constant data, anisotropic thermal parameters, and H atom positions and sample absorbance plots and, for $[PPN][Mn(CO)_4(PEt_3)]\cdot THF$, tables of anisotropic thermal parameters and H atom positions (14 pages); listings of observed and calculated structure factors for $[PPN^+][Mn(CO)_5^-]$ and $[PPN][Mn(CO)_4(PEt_3)]\cdot THF$ (37 pages). Ordering information is given on any current masthead page.

Kinetics and Mechanisms of CO Substitution of $(\eta^5\text{-Ind})Re(CO)_3$ (Ind = Indenyl) with Phosphines and Phosphites. The Indenyl Ligand Effect on Related Trindenylmetal Carbonyls

Hyochoon Bang,[†] Thomas J. Lynch,*[,‡,§] and Fred Basolo*[,†]

Departments of Chemistry, Northwestern University, Evanston, Illinois 60208-3113, and University of Nevada, Reno, Nevada 89557-0020

Received May 14, 1991

Kinetic studies were performed for the reactions of $(\eta^5\text{-Ind})Re(CO)_3$ with phosphines and phosphites. Second-order rate laws were observed, which are first-order in metal complex and first-order in phosphine concentrations. Depending on reaction conditions, i.e., temperature and ligand concentration, two different types of products, $(\eta^1\text{-Ind})Re(CO)_3L_2$ and $(\eta^5\text{-Ind})Re(CO)_2L$, were observed. The η^1-product changed slowly to η^5-product at high temperature. A reaction mechanism which requires a common intermediate for the formation of η^1- and η^5-products is proposed, which allows for simulated spectral changes in accord with what is observed experimentally. Also the reactivity of related trindenyl analogues were compared with indenyl- and cyclopentadienylmetal carbonyl complexes. The rates of reaction follow the order $(\eta^5\text{-Ind})M(CO)_n > (\eta^5\text{-Td})[M(CO)_n]_3 > (\eta^5\text{-Cp})Mo(CO)_n$, where M = Rh ($n = 2$) and Re and Mn ($n = 3$). For a given cyclic ligand, the rates decrease in the order Rh > Re > Mn; for changes in the number of $Re(CO)_3$ groups on a trindenyl ligand, the rates decrease in the order $(\eta^5\text{-TdH}_2)Re(CO)_3 > (\eta^5\text{-TdH})[Re(CO)_3]_2 > (\eta^5\text{-Td})[Re(CO)_3]_3$. These relative rates of reaction are discussed in terms of the coordination number of the metal, its size, and the extent of π-delocalization of electron density in the transition state for reaction.

Introduction

We reported[1] in 1966 our observations that certain 18-electron organometallic compounds readily undergo associative ligand substitution, providing it is possible to localize a pair of electrons on one of the ligands in order to permit reaction via an 18-electron transition state/active intermediate. Reported in the same year was the ligand NO,[1a] which does this by the formation of sp^2 bent nitrosyl, and cyclopentadienyl[1b] and arene[1c] ligands, which involve "ring-slippage" mechanisms.[2] Many examples of this η^5

[†] Northwestern University.
[‡] University of Nevada.
[§] Present address: Hoechst-Celenese, 500 Washington St., Coventry, RI 02816.

(1) (a) Thorsteinson, E. M.; Basolo, F. *J. Am. Chem. Soc.* **1966**, *88*, 3929. (b) Schuster-Woldan, H. G.; Basolo, F. *J. Am. Chem. Soc.* **1966**, *88*, 1657. (c) Zingales, F.; Chiesa, A.; Basolo, F. *J. Am. Chem. Soc.* **1966**, *88*, 2707.

0276-7333/92/2311-0040$03.00/0